Interferometry for electromagnetic transients and noise recordings in lossy media

Evert Slob, Deyan Draganov and Kees Wapenaar

Delft University of Technology, Department of Geotechnology, e.c.slob@tudelft.nl

ABSTRACT

For lossless media, time reversal invariance has been used, by many researchers in different forms and in various acoustic disciplines, to show that the cross-correlation of acoustic wave fields recorded by two different receivers yields the response at one of the receiver positions as if there were a source at the other. Recently, it has been shown for electromagnetic waves using cross-correlation of two recordings in lossless media.

Green's functions representations based on reciprocity relations of the time-correlation type can be approximated to yield accurate results provided the two receivers are in the domain surrounded by sources on a closed surface, while the medium outside this surface is homogeneous. Inside the domain the medium can be arbitrarily heterogeneous but lossless. Non-physical events are introduced outside the time window of interest and they disappear when the sources are located on a surface that is sufficiently irregular. We show in this paper that, for configurations where a medium is lossless inside the domain surrounded by the sources and lossy outside the domain, in theory it is possible to generate cross-correlation results that remain valid for media showing relaxation. Again, non-physical events are introduced that vanish when the sources are located on a surface that is sufficiently irregular. This result can be used in the configuration where two receivers inside the domain and in the situation with one receiver inside and the other outside the domain. These representations can be used for transient and noise recordings.

KEY WORDS: interferometry, lossy media, radar, crosscorrelation, electromagnetic fields.

INTRODUCTION

Passive radar techniques have been used for localization of electromagnetic fields (Knapp *et al.*, 1976), or for radiometry applications, e.g., for Earth observation (Ruf *et al.*, 1988). In this paper we extend the use of interferometric techniques and adopt the notion of interferometry introduced by Schuster (2001) to include the creation of new data. For instantaneously reacting media this concept is known since 1968 when Claerbout (1968) showed that the autocorrelation of an acoustic plane wave transmission response recorded in a one-dimensional configuration at the pressure-free surface yields the reflection response at the pressure-free surface. Weaver and Lobkis (2001) showed that for diffuse wave fields in lossless media the autocorrelation function of an acoustic wave field response is the wave field response of a direct pulse-echo experiment in a three-dimensional configuration. Based on the diffusivity of the wave field, many authors showed similar results also for crosscorrelations in open and closed configurations (e.g. Lobkis and Weaver, 2001, Campillo and Paul, 2003, van Tiggelen, 2003}. Later it was shown for deterministic instantaneously reacting media that Claerbout's principle could be extended to three-dimensional media (Wapenaar *et al.*, 2002, Derode *et al.*, 2003). Recently, it has been shown that similar representations can be derived for electromagnetic waves in lossless media (Slob *et al.*, 2006a,b).

Here we use reciprocity theorems of the time-correlation type (Bojarski, 1983) as point of departure for our derivations and derive interferometric representations for the electric field Green's function for an electric current source in new configurations. The configuration is a bounded domain with a closed surface at which sources are active. We look at different locations of the receivers, either both inside this bounded domain or with one receiver inside and the other outside this domain. These two recordings can be crosscorrelated. The result is independent of the location of the closed boundary and independent of the sources. It then represents the field as if it were generated at one of the two recording locations and received at the other location together with its time-reversed version. These representations are only valid when the media inside the domain are instantaneously reacting media, since time-reversal invariance relies on the conservation of total wave energy. Known representations use configurations where it is assumed that the medium outside the domain of reciprocity is homogeneous and lossless. We show here that interferometry by crosscorrelation leads to exact representations of the Green's function for lossy media when the losses occur only outside the domain of reciprocity. These representations can be used for any electromagnetic method, hence apart from radar also for induction type methods like seabed logging and magneto-telluric methods.

RECIPROCITY

We use the subscript notation to denote tensors and the summation convention applies to repeated subscripts. The electric field is given by $E_k(\boldsymbol{x},t)$, the magnetic field is denoted $H_j(\boldsymbol{x},t)$, while the sources of the electric and magnetic current types are $J_k^e(\boldsymbol{x},t), J_k^m(\boldsymbol{x},t)$. The medium is characterized in terms of the electric and magnetic conductivities, $\eta_{kr}(\boldsymbol{x},t), \zeta_{jp}(\boldsymbol{x},t)$, which include the electric permittivity and magnetic permeability. Their two subscripts indicate that we assume anisotropic media. We define the Fourier transform of a time domain function as

$$\hat{E}_k(\boldsymbol{x},\omega) = \int_{t=0}^{\infty} E_k(\boldsymbol{x},t)\exp(-j\omega t)dt \,, \tag{1}$$

where j is the imaginary unit and ω denotes angular frequency.

In space-fequency domain the Maxwell equations in matter are given by

$$\begin{aligned} -\in_{mkj}\ \partial_m \hat{H}_j(\mathbf{x},\omega) + \hat{\eta}_{kr}(\mathbf{x},\omega)\hat{E}_r(\mathbf{x},\omega) &= -\hat{J}^e_k(\mathbf{x},\omega), \\ \in_{jnr}\ \partial_n \hat{E}_r(\mathbf{x},\omega) + \hat{\zeta}_{jp}(\mathbf{x},\omega)\hat{H}_p(\mathbf{x},\omega) &= -\hat{J}^m_j(\mathbf{x},\omega), \end{aligned} \tag{2}$$

where the generalized electric and magnetic conductivities are given by

$$\begin{aligned} \hat{\eta}_{kr}(\mathbf{x},\omega) &= j\omega\varepsilon_{kr}(\mathbf{x}) + \hat{\sigma}^e_{kr}(\mathbf{x},\omega), \\ \hat{\zeta}_{jp}(\mathbf{x},\omega) &= j\omega\mu_{jp}(\mathbf{x}) + \hat{\sigma}^m_{jp}(\mathbf{x},\omega). \end{aligned} \tag{3}$$

Note that we can take the electric permittivity and magnetic permeability, $\varepsilon_{kr}(\boldsymbol{x}), \mu_{jp}(\boldsymbol{x})$, as frequency independent functions without loss of generality, because the relaxation or other loss mechanism can be fully included in the electric and magnetic conductivities, viz. $\hat{\sigma}^e_{kr}(\boldsymbol{x},\omega), \hat{\sigma}^m_{jp}(\boldsymbol{x},\omega)$.

For time-correlation type reciprocity representation we need the time-reversed or complex conjugate in the frequency domain, Maxwell equations

$$\begin{aligned} -\in_{mkj}\ \partial_m \hat{H}^*_j(\mathbf{x},\omega) + \hat{\eta}^*_{kr}(\mathbf{x},\omega)\hat{E}^*_r(\mathbf{x},\omega) &= -\hat{J}^{e*}_k(\mathbf{x},\omega) \\ \in_{jnr}\ \partial_n \hat{E}^*_r(\mathbf{x},\omega) + \hat{\zeta}^*_{jp}(\mathbf{x},\omega)\hat{H}^*_p(\mathbf{x},\omega) &= -\hat{J}^{m*}_j(\mathbf{x},\omega) \end{aligned} \tag{4}$$

The reciprocity relation is obtained by considering two not necessarily identical states, labeled A and B, that occupy the same domain in space. Their material properties need not be the same nor their sources and fields. A representation considering vanishing sources of the magnetic current type is used here together with the assumption that the media in the states A and B are the same, $\hat{\eta}_{kr,A}(\boldsymbol{x},\omega) = \hat{\eta}_{kr,B}(\boldsymbol{x},\omega), \hat{\zeta}_{jp,A}(\boldsymbol{x},\omega) = \hat{\zeta}_{jp,B}(\boldsymbol{x},\omega)$, and the additional assumption that both states are self-adjoint. The domain to which we apply reciprocity is a bounded domain, $\mathbb{D}$, with closed boundary surface, $\partial\mathbb{D}$ and a unique outward pointing unit normal, $\boldsymbol{n}$. If we use the causal state for state B and the time-reversed state for state A, we obtain the reciprocity relation of the time-correlation type,

$$\begin{aligned} &\oint_{\mathbf{x}\in\partial\mathbb{D}} \in_{mkj}\ n_m \left(\hat{E}^*_{r,A}\hat{H}_{j,B} + \hat{E}_{r,B}\hat{H}^*_{j,A}\right) d^2\mathbf{x} = \\ &-\int_{\mathbf{x}\in\mathbb{D}} \left(\hat{E}^*_{r,A}\Re\left\{\hat{\sigma}^e_{kr}\right\}\hat{E}_{r,B} + \hat{H}^*_{j,A}\Re\left\{\hat{\sigma}^m_{kr}\right\}\hat{H}_{r,B}\right) d^3\mathbf{x} \\ &\quad -\int_{\mathbf{x}\in\mathbb{D}} \left(\hat{J}^{e*}_{r,A}\hat{E}_{r,B} + \hat{J}^e_{r,B}\hat{E}^*_{r,A}\right) d^3\mathbf{x}. \end{aligned} \tag{5}$$

In these representations the magnetic field occur, which can be eliminated using the second Maxwell equation. The presence of the electric and magnetic conductivities in equation (5) is undesired. It implies that in case the media show relaxation inside the domain where reciprocity has been applied, this volume integral contributes to the final result. For interferometric purposes it is an unknown factor that we cannot easily determine by other means. For more detailed discussions on the reciprocity theorems we refer to de Hoop (1995).

INTERFEROMETRIC REPRESENTATIONS

Here we assume that the media inside the domain $\mathbb{D}$ are instantaneously reacting and only show relaxation and other loss mechanisms in the complement of $\mathbb{D}$. We further assume that the media in the neighborhood of the boundary $\partial\mathbb{D}$ are homogeneous and isotropic. It can then be shown that equation (5) reduces to

$$\begin{aligned} &\frac{1}{j\omega\mu}\oint_{\mathbf{x}\in\partial\mathbb{D}} \left(\hat{E}^*_{r,A} n_m \partial_m \hat{E}_{r,B} - \hat{E}_{r,B} n_m \partial_m \hat{E}^*_{r,A}\right) d^2\mathbf{x} = \\ &\int_{\mathbf{x}\in\mathbb{D}} \left(\hat{J}^{e*}_{r,A}\hat{E}_{r,B} + \hat{J}^e_{r,B}\hat{E}^*_{r,A}\right) d^3\mathbf{x}. \end{aligned} \tag{6}$$

These representations form the basis of our development. We now specify receiver locations by making choices for the sources in equation (6). In equation (6) it can be seen that the right-hand side vanished when both receivers are located outside domain $\mathbb{D}$.

Both receivers inside $\mathbb{D}$

We define the observation points by taking the points $\boldsymbol{x}_A$ and $\boldsymbol{x}_B$ as source point locations for the sources in states A and B such that both $\boldsymbol{x}_A$ and $\boldsymbol{x}_B$ lie inside the domain $\mathbb{D}$. Then the fields reduce to Green's functions and are given by

$$\begin{aligned} \hat{J}^e_{k,A} &= \delta_{kr}\delta(\mathbf{x}-\mathbf{x}_A), \hat{E}_{r,A} = \hat{G}_{rk}(\mathbf{x},\mathbf{x}_A,\omega), \\ \hat{J}^e_{k,B} &= \delta_{kr}\delta(\mathbf{x}-\mathbf{x}_B), \hat{E}_{r,B} = \hat{G}_{rk}(\mathbf{x},\mathbf{x}_B,\omega). \end{aligned} \tag{7}$$

Substituting the expressions of equation (7) in equation (6) results in an exact representation of the electric field Green's function

$$2\Re\left\{\hat{G}_{kr}(\mathbf{x}_A,\mathbf{x}_B,\omega)\right\} =$$
$$-\frac{1}{j\omega\mu}\oint_{\mathbf{x}\in\partial\mathbb{D}}\Big(\hat{G}^*_{kj}(\mathbf{x}_A,\mathbf{x},\omega)n_m\partial_m\hat{G}_{rj}(\mathbf{x}_B,\mathbf{x},\omega)$$
$$-\hat{G}_{rj}(\mathbf{x}_B,\mathbf{x},\omega)n_m\partial_m\hat{G}^*_{kj}(\mathbf{x}_A,\mathbf{x},\omega)\Big)d^2\mathbf{x}. \quad (8)$$

This representation is exact for lossy media, where the media can be arbitrarily heterogeneous and anisotropic outside and inside $\mathbb{D}$, as long as all loss mechanisms occur in the complement of $\mathbb{D}$ only. Summing the crosscorrelations, of recorded fields at two locations inside $\mathbb{D}$, over all sources located on the boundary surface yields the exact real part of the electric field Green's function as if there were a source in $\boldsymbol{x}_B$ and the receiver in $\boldsymbol{x}_A$. In the time domain, this is equivalent to constructing the causal Green's function and its time reversed version, which do not overlap except possibly at $t=0$.

One receiver inside and one outside $\mathbb{D}$

We define the observation points by taking the points $\boldsymbol{x}_A$ and $\boldsymbol{x}_B$ as source point locations for the sources in states A and B such that $\boldsymbol{x}_A$ is inside and $\boldsymbol{x}_B$ lies outside the domain $\mathbb{D}$. Again the fields reduce to Green's functions. Now both convolution and correlation type representations can be used and lead to

$$\hat{G}_{kr}(\mathbf{x}_A,\mathbf{x}_B,\omega) =$$
$$-\frac{1}{j\omega\mu}\oint_{\mathbf{x}\in\partial\mathbb{D}}\Big(\hat{G}^*_{kj}(\mathbf{x}_A,\mathbf{x},\omega)n_m\partial_m\hat{G}_{rj}(\mathbf{x}_B,\mathbf{x},\omega)$$
$$-\hat{G}_{rj}(\mathbf{x}_B,\mathbf{x},\omega)n_m\partial_m\hat{G}^*_{kj}(\mathbf{x}_A,\mathbf{x},\omega)\Big)d^2\mathbf{x}. \quad (9)$$

Although the right-hand side of equation (9) looks very similar to the right-hand side of equation (8), their left-hand sides differ. Now we construct the complex Green's function, which leads to the causal Green's function in the time domain. Also this representation is an exact result under the same conditions that applied to the validity of equation (8).

SIMPLIFIED REPRESENTATIONS

The integrands in the representations of equations (8) and (9) can be understood as contributions from dipole and quadrupole sources. In practice dipole sources exist and are used, while quadrupole sources are not easily found. To be able to understand equations (8) and (9) as correlations of electric field recordings we must find suitable approximations for the normal derivative that occurs in the right-hand side of equations (8) and (9). Since we use the representations here with heterogeneities and loss mechanisms outside the domain $\mathbb{D}$, we must first specify where these heterogeneities occur relative to the location of the domain $\mathbb{D}$. We take the domain $\mathbb{D}$ such that the domain containing all heterogeneities and loss mechanisms are separated such that a plane exists that does not intersect the two domains, see Figure 1. For simplicity we take the domain $\mathbb{D}$ to have flat boundaries that extend to "infinity", such that the closing sides at "infinity" have a vanishing contribution. The boundaries of the domain are indicated by the dashed and solid lines. Above the dashed line (in the negative x_3-direction) the medium is homogeneous, isotropic and instantaneously reacting, while below it (in the positive x_3-direction) the medium is arbitrarily heterogeneous, anisotropic and lossy.

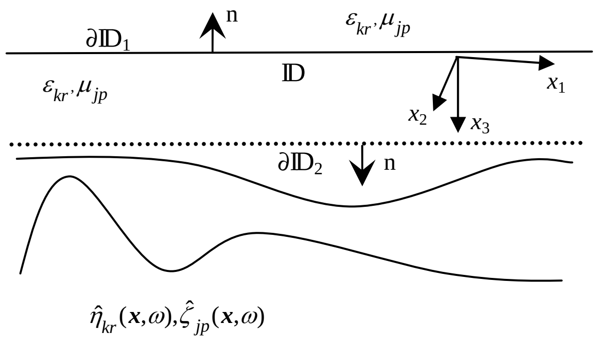

Figure 1. The configuration for interferometry with heterogeneities and loss mechanisms outside the domain $\mathbb{D}$.

In this configuration and for observation points below the dashed line only waves that travel in a direction with a non-zero component in the positive x_3-direction contribute to the measurement. For sources located on the dashed line only outgoing waves contribute the measurement. For observation points above the dashed line, both ingoing and outgoing waves that are generated by the sources on the dashed line contribute to the measurement. For sources on the solid line similar arguments hold for observation points above or below the solid line.

Both receivers inside $\mathbb{D}$

When we take both receivers inside the domain $\mathbb{D}$, only ingoing waves from the top boundary contribute and we can make a high-frequency far-field approximation for the differentiations in the right-hand side of equation (8). This leads to $n_m\partial_m \approx -j\omega|\cos(\alpha(\boldsymbol{x}))|/c$, where c denotes the wave velocity and $\alpha(\boldsymbol{x})$ denotes the angle of emission a generalized ray makes with the unit normal of the boundary surface. The situation for the contributions from the bottom boundary (dashed line in Figure 1) is more complicated. Generalized rays that leave the boundary as ingoing waves contribute to the direct wave in the end result that corresponds to the wave that travels between the two receivers. Generalized rays that leave the boundary as ingoing waves that are recorded at $\boldsymbol{x}_A$ and that are correlated with generalized rays that leave the boundary as outgoing waves and are recorded at $\boldsymbol{x}_B$ lead to non-physical arrivals. These arrivals are canceled in equation (8) because the two terms in the right-hand side of equation (8) ensures cancellation of correlations of ingoing and outgoing waves. The reason is that the points along the boundary that contribute to these results are stationary points (Schuster *et al.*, 2004 and Snieder, 2004). At those points the absolute ray angles for the Green's functions of both states are identical. Generalized rays that leave the boundary as outgoing waves contribute to the Green's function. Also for contributions from this boundary a high-frequency far-field approximation is made favoring the physical events, hence we take $n_m\partial_m \approx j\omega|\cos(\alpha(\mathbf{x}))|/c$. Assuming for both boundary surfaces the major contribution comes from generalized rays leaving the boundary surface perpendicularly, we take $\alpha(\mathbf{x}) = 0$ and obtain

$$\Re\left\{\hat{G}_{kr}(\mathbf{x}_A,\mathbf{x}_B,\omega)\right\} \approx \frac{1}{\mu c}\oint_{\mathbf{x}\in\{\partial\mathbb{D}_1+\partial\mathbb{D}_2\}} \hat{G}^*_{kj}(\mathbf{x}_A,\mathbf{x},\omega)\hat{G}_{rj}(\mathbf{x}_B,\mathbf{x},\omega)d^2\mathbf{x}. \tag{10}$$

Equation (10) is an approximate expression that is acceptable for electromagnetic interferometry in situations where the media show relaxation or other type of loss mechanisms outside the domain spanned by the sources. Due to the approximation, non-physical events are introduced in the time window of interest, which is in principle a serious problem. The physical events are part of the Green's function and therefore their result is independent on the location of the sources on the boundary surfaces. The non-physical events are events that are not part of the Green's function and do depend on the location of the sources on the boundary surface. This implies that when the surface has a sufficiently irregular shape, the non-physical events are cancelled by destructive interference. This has been first shown numerically by Draganov *et al.* (2004). The accuracy of the approximation of the physical events depends very much on the heterogeneity of the medium.

One receiver inside and one outside $\mathbb{D}$

When we take one receiver inside the domain $\mathbb{D}$ and one outside the argumentation that follows depends on whether the location outside is in between the domain and the heterogeneous medium or whether it is located at larger negative depth values compared to the domain $\mathbb{D}$. We take here the point $\boldsymbol{x}_B$, to be located in between the domain and the heterogeneous medium. Then the situation for the top boundary (solid line in Figure 1) is unchanged compared to the situation with both receivers inside the domain. This leads again to the approximation $n_m\partial_m \approx -j\omega|\cos(\alpha(\mathbf{x}))|/c.$ The situation for the bottom boundary (dashed line in Figure 1) is slightly changed. Generalized rays that leave the boundary as ingoing or outgoing waves are recorded at $\boldsymbol{x}_A$ and that are correlated with generalized rays that leave the boundary as outgoing waves and are recorded at $\boldsymbol{x}_B$ lead to both physical and non-physical arrivals. Also here we use the destructive interference effect of an irregularly shaped boundary surface for contributions from this boundary and apply a high-frequency far-field approximation, favoring the physical events, hence we take $n_m\partial_m \approx j\omega|\cos(\alpha(\mathbf{x}))|/c$. Assuming for both boundary surfaces the major contribution comes from generalized rays leaving the boundary surface perpendicularly, we take $\alpha(\boldsymbol{x}) = 0$ and obtain

$$\hat{G}_{kr}(\mathbf{x}_A,\mathbf{x}_B,\omega) \approx \frac{2}{\mu c}\oint_{\mathbf{x}\in\{\partial\mathbb{D}_1+\partial\mathbb{D}_2\}} \hat{G}^*_{kj}(\mathbf{x}_A,\mathbf{x},\omega)\hat{G}_{rj}(\mathbf{x}_B,\mathbf{x},\omega)d^2\mathbf{x}. \tag{11}$$

Equation (11) is an approximate expression that is acceptable for electromagnetic interferometry in situations where the media show relaxation or other type of loss mechanisms outside the domain spanned by the sources.

TRANSIENT AND NOISE SOURCES

In situations where transient sources are used we can define measured electric fields as

$$\begin{aligned}\hat{E}^{\text{obs}}_{kj}(\boldsymbol{x}_A,\boldsymbol{x},\omega) &= \hat{G}_{kj}(\boldsymbol{x}_A,\boldsymbol{x},\omega)\hat{s}^{(j)}(\boldsymbol{x},\omega),\\ \hat{E}^{\text{obs}}_{rj}(\boldsymbol{x}_B,\boldsymbol{x},\omega) &= \hat{G}_{rj}(\boldsymbol{x}_B,\boldsymbol{x},\omega)\hat{s}^{(j)}(\boldsymbol{x},\omega),\end{aligned} \tag{12}$$

where $\hat{s}^{(j)}(\boldsymbol{x},\omega)$ is the source frequency spectrum in the $\boldsymbol{x}_j$–direction at position $\boldsymbol{x}$, which can be different for each source position. To express the Green's function of equations (10) and (11) in terms of these measured electric fields we introduce the power spectrum of the sources and a shaping filter as

$$\begin{aligned}\hat{S}^{(j)}(\boldsymbol{x},\omega) &= \hat{s}^{(j)*}(\boldsymbol{x},\omega)\hat{s}^{(j)}(\boldsymbol{x},\omega),\\ \hat{F}^{(j)}(\boldsymbol{x},\omega) &= \hat{S}_0(\omega)\Big/\Big[\mu c\hat{S}^{(j)}(\boldsymbol{x},\omega)\Big],\end{aligned} \tag{13}$$

where $\hat{S}_0(\omega)$ denotes a desired source spectrum. Using these definitions in equations (10) and (11) we find

$$\begin{aligned}\Re\left\{\hat{G}_{kr}(\mathbf{x}_A,\mathbf{x}_B,\omega)\right\}\hat{S}_0(\omega) \approx \oint_{\mathbf{x}\in\{\partial\mathbb{D}_1+\partial\mathbb{D}_2\}} &\hat{F}^{(j)}(\mathbf{x},\omega)\\ &\times\hat{E}^{\text{obs}*}_{kj}(\mathbf{x}_A,\mathbf{x},\omega)\hat{E}^{\text{obs}}_{kj}(\mathbf{x}_B,\mathbf{x},\omega)d^2\mathbf{x},\end{aligned} \tag{14}$$

when both $\boldsymbol{x}_A$ and $\boldsymbol{x}_B$ are located inside $\mathbb{D}$, while

$$\begin{aligned}\hat{G}_{kr}(\mathbf{x}_A,\mathbf{x}_B,\omega)\hat{S}_0(\omega) \approx 2\oint_{\mathbf{x}\in\{\partial\mathbb{D}_1+\partial\mathbb{D}_2\}} &\hat{F}^{(j)}(\mathbf{x},\omega)\\ &\times\hat{E}^{\text{obs}*}_{kj}(\mathbf{x}_A,\mathbf{x},\omega)\hat{E}^{\text{obs}}_{kj}(\mathbf{x}_B,\mathbf{x},\omega)d^2\mathbf{x},\end{aligned} \tag{15}$$

when $\boldsymbol{x}_A$ is located inside and $\boldsymbol{x}_B$ is outside $\mathbb{D}$.

In case of uncorrelated noise sources we use the following definition for the sources

$$\left\langle N_j^*(\boldsymbol{x},\omega)N_p(\boldsymbol{x}',\omega)\right\rangle = \delta_{jp}\delta(\boldsymbol{x}-\boldsymbol{x}')\hat{S}(\omega)\big/\mu c. \quad (16)$$

The observed electric fields are now written as integrals over all the sources as

$$\begin{aligned}\hat{E}_{kj}^{\text{obs}}(\boldsymbol{x}_A,\omega) &= \int_{\boldsymbol{x}\in\partial ID}\hat{G}_{kj}(\boldsymbol{x}_A,\boldsymbol{x},\omega)N_j(\boldsymbol{x},\omega)d^2\boldsymbol{x},\\ \hat{E}_{rj}^{\text{obs}}(\boldsymbol{x}_B,\omega) &= \int_{\boldsymbol{x}\in\partial ID}\hat{G}_{kj}(\boldsymbol{x}_B,\boldsymbol{x},\omega)N_j(\boldsymbol{x},\omega)d^2\boldsymbol{x},\end{aligned} \quad (17)$$

which leads to

$$\Re\left\{\hat{G}_{kr}(\mathbf{x}_A,\mathbf{x}_B,\omega)\right\}\hat{S}(\omega) \approx \left\langle \hat{E}_{kj}^{\text{obs}*}(\mathbf{x}_A,\omega)\hat{E}_{kj}^{\text{obs}}(\mathbf{x}_B,\omega)\right\rangle, \quad (18)$$

when both $\boldsymbol{x}_A$ and $\boldsymbol{x}_B$ are located inside $\mathbb{D}$, while

$$\hat{G}_{kr}(\mathbf{x}_A,\mathbf{x}_B,\omega)\hat{S}(\omega) \approx 2\left\langle \hat{E}_{kj}^{\text{obs}*}(\mathbf{x}_A,\omega)\hat{E}_{kj}^{\text{obs}}(\mathbf{x}_B,\omega)\right\rangle, \quad (19)$$

when $\boldsymbol{x}_A$ is located inside and $\boldsymbol{x}_B$ is outside $\mathbb{D}$.

NUMERICAL RESULTS

To show the accuracy of the derived approximate expressions we use a two-dimensional configuration consisting of two boundaries, both in the air, containing the sources. Below the bottom boundary a two-layered, lossy, medium is present, see Figure 2. Two receiver configurations are used. In the first both receivers are located inside the domain and in the second one is inside and one is outside the domain. In the latter configuration, the receiver outside the domain is located at the earth surface, hence in between the domain and the layered medium, as indicated in Figure 2.

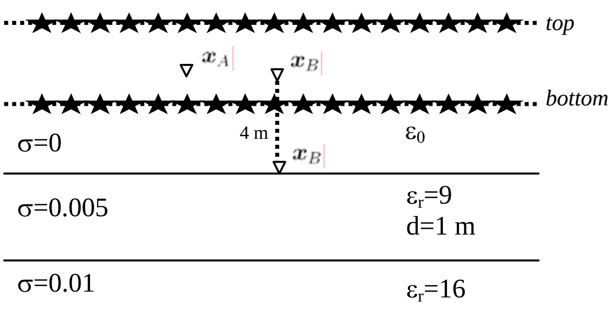

Figure 2. The configuration for the numerical results, both boundary surfaces are located in the air, above a two-layered medium. Two receivers are inside the domain and a configuration where one receiver is inside and the other is outside the domain.

The first example shows a common-shot gather, with an initial horizontal offset of 1.5 m and zero vertical offset. Both receivers are located 4 m above the ground surface, while the bottom boundary and the top boundary containing the sources are located at 2 m and 6 m above the ground surface, respectively. The horizontal distance between the sources is 0.2 m, which distance is also taken for the receivers to generate the shot-gathers with. We have used a total of 256 sources spanning a total width of 51 m.

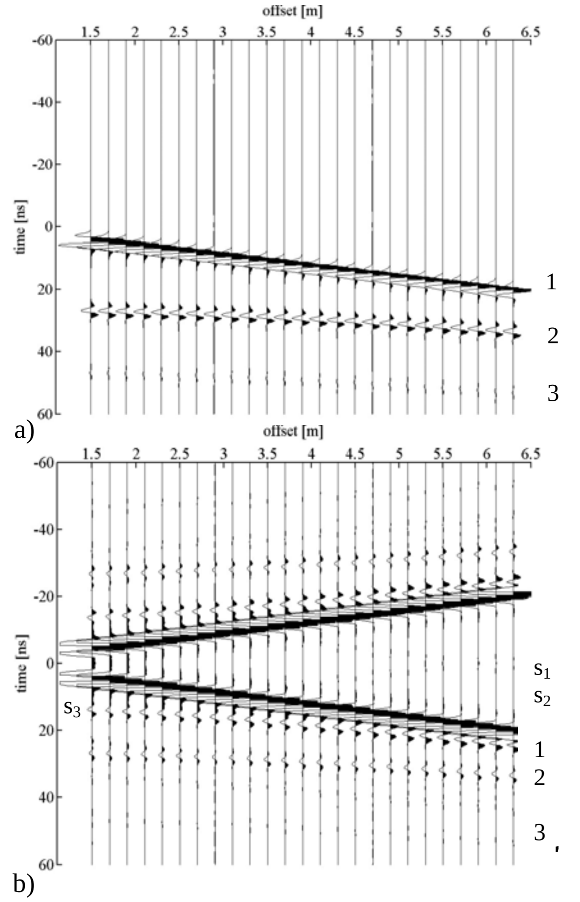

Figure 3. Shot-gather with initial horizontal offset of 1.5 m and 20 cm increments corresponding to the model configuration of Figure 2, with both receivers inside the domain $\mathbb{D}$, directly modeled in a) and the correlation result in b). Physical events are numbered 1, 2 and 3, while the non-physical events are numbered s_1, s_2 and s_3.

The directly modeled result is shown in Figure 3a, while the result obtained with crosscorrelation is shown in Figure 3b. The three physical events, labeled 1, 2 and 3, are modeled with the correct amplitudes, but three non-physical events are observed and indicated in the figure as s_1, s_2 and s_3. Both physical and non-physical events occur in time-symmetric form around $t = 0$, as expected. The non-physical events are eliminated when the shapes of the boundary surfaces are sufficiently irregular.

When we take a common-shot gather with one receiver inside and one outside $\mathbb{D}$ as a second example the crosscorrelation result should produce the causal Green's function, which be compared with the directly modeled result. We take now one receiver located on top of the ground surface and the other receiver at 4m above the ground surface. The crosscorrelation result is shown in Figure 4. All physical events, labeled 1 and 2, are obtained with the correct arrival time and amplitude. The interesting feature of the non-physical events, labeled s_1 and s_2, is that they occur in time-symmetric form around their zero horizontal offset arrival time. This implies that they can be identified in shot gathers or common midpoint gathers. They also disappear when the shapes of the boundary surfaces are sufficiently irregular.

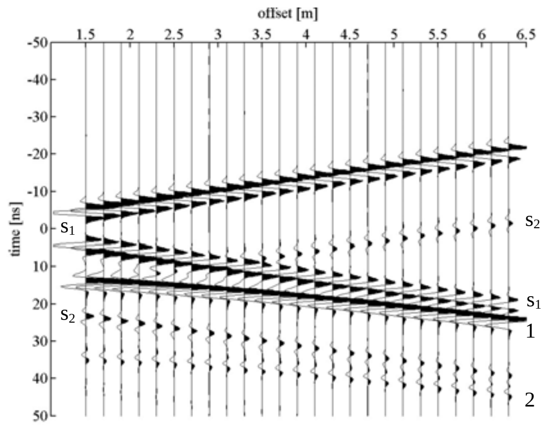

Figure 4. The crosscorrelation result for one receiver inside and one outside the domain, with a vertical offset of 4 m and a horizontal offset of 1.5 m. Physical events are labeled 1 and 2, while the non-physical events are labeled s_1, s_2.

CONCLUSIONS

We have shown that exact representations of Green's functions of lossy, heterogeneous, anisotropic media can be derived using crosscorrelation type of interferometry. The condition is that the medium inside the domain spanned by the sources is lossless. Approximate expressions for the Green's function are obtained with the additional conditions that the domain spanned by the sources is completely located in a homogeneous and lossless embedding such that there exist a plane, in the homogeneous and lossless embedding, that does not intersect the heterogeneous and lossy medium. Then the approximate representations yield accurate results for the physical events, but additional non-physical events occur in the correlation results. When both receivers are located inside the domain all events are time-symmetric relative to time-zero. In this situation the non-physical events are eliminated when the boundary shape is sufficiently irregular. When one receiver is inside and one is outside the domain the causal Green's function is obtained and the introduced non-physical events are easily identified because they occur in time-symmetric form relative to their zero-offset arrival time.

ACKNOWLEDGEMENTS

This work is part of the research program of the Netherlands research center for Integrated Solid Earth Science (ISES). The research of DD is supported by the Dutch Technology Foundation, STW, under project number DET4915.

REFERENCES

Bojarski, N., 1983, Generalized reaction principles and reciprocity theorems for the wave equations, and the relationships between time-advanced and time-retarded fields, *JASA*, **74**, 281-285.

Campillo, M. and Paul, A., 2003, Long-range correlations in the diffuse seismic coda waves, *Science*, **299**, 547-549.

Claerbout, J., 1968, Synthesis of a layered medium from its acoustic transmission response, *Geophysics*, **33**, 264-269.

Derode, A., Larose, E., Tanter, M., de Rosny, J., Tourin, A., Campillo, M. and Fink, M., 2003, Recovering the Green's function from field-field correlations in an open scattering medium (L), *JASA*, **113**, doi:10.1121/1.1570436.

Draganov, D., Wapenaar, C.P.A., and Thorbecke, J., 2001, Passive seismic imaging in the presence of white noise sources, *The Leading Edge*, **23**, 889-892.

de Hoop, A.T., 1995, *Handbook of radiation and scattering*, Academic Press, Amsterdam.

Knapp, C.H. and Carter, G.C., 1976, The generalized correlation method for estimating time delay, *IEEE Trans. on Acoust. Speech, Signal Processing*, **24**, 320-327.

Lobkis, O. and Weaver, R., 2001, On the emergence of the Green's function in the correlations of a diffuse field, *JASA*, **110**, 3011-3017.

Ruf, C.S. Swift, C.T., Tanner, A.B. and le Vine, D.M., 1988, Interferometric synthetic aperture microwave radiometry for the remote sensing of the Earth, *IEEE Trans. on Geosci. Remote Sensing* ,**26**, 597-611.

Slob, E., Draganov, D. and Wapenaar, K., 2006a, GPR without a source, 11th International Conference on GPR, Ohio State University, Proceedings, ANT.6.

Slob, E., Draganov, D. and Wapenaar, K., 2006b, Let the FCC rules work for you: turning commercial noise into useful data, 11th International Conference on GPR, Ohio State University, Proceedings, AIR.5.

Schuster, G., 2001, Theory of daylight/interferometric imaging: tutorial, 63rd Ann International Meeting, Eur. Assoc. Geosci. & Eng., Extended Abstract, A32.

Schuster, G.T., Yu, J., Sheng, J. and Ricket, J., 2001, Interferometric/daylight seismic imaging, *Geophys. Journal International*, **157**, 838-852.

Snieder, R., 2004, Extracting the Green's function from the correlation of coda waves: A derivation based on stationary phase, Phys, Rev. E

Wapenaar, C., Draganov, D., Thorbecke, J. and Fokkema, J., Theory of acoustic daylight imaging revisited, 72nd Ann International Meeting, Soc. Expl. Geophys., Expanded Abstract, 2269-2272.

Weaver, R. and Lobkis, O., 2001, Ultrasonics without a source: Thermal fluctuation correlations at MHz frequencies, *Phys. Rev. Lett.*, **87**, doi:10.1103/PhysRevLett.87.134301.